

## Chapter 5

### Fractal Parameter Space of Lorenz-like Attractors: A Hierarchical Approach

Tingli Xing

*Department of Mathematics and Statistics,  
Georgia State University, Atlanta, GA 30303, USA  
txing1@student.gsu.edu*

Jeremy Wojcik

*Applied Technology Associates, Albuquerque,  
New Mexico, 87123, USA  
wojcik.jeremy@gmail.com*

Michael A. Zaks

*Institute of Mathematics, Humboldt University of Berlin,  
Berlin, 12489, Germany  
zaks@mathematik.hu-berlin.de*

Andrey Shilnikov

*Neuroscience Institute and Department of Mathematics and Statistics,  
Georgia State University, Atlanta, GA 30303, USA  
and Department of Computational Mathematics and Cybernetics,  
Lobachersky State University of Nizhni Novgorod,  
Nizhni Novgorod, Russia  
ashilnikov@gsu.edu*

Using bi-parametric sweeping based on symbolic representation we reveal self-similar fractal structures induced by hetero- and homoclinic bifurcations of saddle singularities in the parameter space of two systems with deterministic chaos. We start with the system displaying a few homoclinic bifurcations of higher codimension: resonant saddle, orbit-flip and inclination switch that all can give rise to the onset of the Lorenz-type attractor. It discloses a universal unfolding pattern in the

case of systems of autonomous ordinary differential equations possessing two-fold symmetry or “ $\mathbb{Z}_2$ -systems” with the characteristic separatrix butterfly. The second system is the classic Lorenz model of 1963, originated in fluid mechanics.

## 1. Introduction

Iconic shape of the Lorenz attractor has long become the emblem of the Chaos theory as a new paradigm in nonlinear sciences. This emblem has been reprinted on innumerable announcing flyers popular lectures and various cross-disciplinary meetings with broad research scopes, as well as on those for specializing workshops with the keen emphasis on dynamical systems, especially applied. The year 2013 was the 50-th anniversary of the original paper by E. Lorenz<sup>1</sup> introducing a basic system of three ordinary differential equations with highly unordinary trajectory behavior — deterministic chaos and its mathematical image — the chaotic attractor. The concept of deterministic chaos illustrated by snapshots of the Lorenz attractor has been introduced in most textbooks on nonlinear dynamics for a couple of last decades at least. Nowadays, the Lorenz attractor is firmly and stereotypically associated with images of chaos, including the celebrated Lorenz 1963 model.

The reference library of publications on the Lorenz model and Lorenz-like systems of various origins is innumerable too. The ideas of this research trend are deeply rooted in the pioneering, chronologically and phenomenologically, studies led by L.P. Shilnikov in the city of Gorky, in USSR.<sup>2-5</sup> His extensive knowledge of the homoclinic bifurcations helped to make the theory of strange attractors a mathematical marvel. Like the most of complete mathematical theories, it started with abstract hypothesis and conjectures, followed by principles and supported by theorems. On the next round, the theory has given rise to the development of computational tools designed for the search and identification of basic invariants to quantify chaotic dynamics. With the help of the current technology (like massively parallel GPUs) calling for new computational approaches, we would like to re-visit [to re-discover] the wonder of the Lorenz model this time viewed not only through the elegant complexity of the behavior of trajectories in the phase space but through disclosing a plethora of fractal-hierarchical organizations of the parameter space of such systems, which were foreseen in the pioneering work of John S. Nicolis.<sup>24,25</sup> In this context John S. Nicolis highlighted the importance of the attractor’s invariant

measure non-uniformity as a key determinant of the information processing by chaotic dynamical systems. Our work is an extension of the earlier paper: “Kneadings, Symbolic Dynamics and Painting Lorenz Chaos” by R. Barrio, A. Shilnikov and L. Shilnikov.<sup>6</sup>

The computational approach we employ for studying systems with complex dynamics capitalizes on one of the key properties of deterministic chaos — the sensitive dependence of solutions on perturbations, like variations of control parameters. In particular, for the Lorenz-type attractors, chaotic dynamics is characterized by unpredictable flip-flop switching between the two spatial wings of the strange attractor, separated by a saddle singularity.

The core of the computational toolkit is the binary,  $\{0, 1\}$ , representation of a single solution — the outgoing separatrix of the saddle as it fills out two symmetric wings of the Lorenz attractor with unpredictable flip-flops patterns (Fig. 2). Such patterns can persist or change with variations of parameters of the system. Realistically and numerically we can access and differentiate between only appropriately long episodes of patterns due to resolution limits (see below). The positive quantity, called the kneading,<sup>7</sup> bearing the information about the pattern, lets one quantify the dynamics of the system. By sweeping bi-parametrically, we find the range of the kneadings. Whenever the kneading value persists within a parameter range, then the flip-flop pattern remains constant thus indicating that dynamics is likely robust (structurally stable) and simple. In the parameter region of the Lorenz attractor, the patterns change constantly but somewhat predictably. Here, the kneading value remains the same along a “continuous” line. Such a line corresponds to a homoclinic bifurcation via a formation of the separatrix loop of the saddle. No such bifurcation curves may cross or merge unless at a singular point corresponding to some homo- or heteroclinic bifurcation of codimension-2 in the parameter plane. As so, by foliating the parameter plane with such multi-colored lines, one can disclose its bifurcation structure and identify its organizing centers.

The kneading invariant<sup>7</sup> was originally introduced as a quantity to describe the complex dynamics of a system that allows a symbolic description in terms of two symbols, as for example on the increasing and decreasing branches separated by the critical point in the 1D logistic map. Two systems with complex dynamics, including ones with the Lorenz attractors, can topologically be conjugate if they have the same kneading invariant.<sup>8–10</sup> The forward flip-flop iterations of the right separatrix,  $\Gamma^+$ , of the saddle in a symmetric system can generate a *kneading sequence*  $\{\kappa_n\}$

as follows:

$$\kappa_n = \begin{cases} +1, & \text{when } \Gamma^+ \text{ turns around the right saddle-focus } O_1, \\ 0, & \text{when } \Gamma^+ \text{ turns around the left saddle-focus } O_2. \end{cases} \quad (1)$$

The kneading invariant for the system is then defined in the form of a formal power series:

$$K(q, \mu) = \sum_{n=0}^{\infty} \kappa_n q^n, \quad (2)$$

convergent if  $0 < q < 1$ . The kneading sequence  $\{\kappa_n\}$  comprised of only +1's corresponds to the right separatrix converging to the right equilibrium state or a stable orbit with  $x(t) > 0$ . The corresponding kneading invariant is maximized at  $\{K_{\max}(q)\} = 1/(1-q)$ . When the right separatrix converges to an  $\omega$ -limit set with  $x(t) < 0$  then the kneading sequence begins with the very first 1 followed by an infinite string of 0's. Skipping the very first same "+1", yields the range,  $[0, q/(1-q)]$ , for the kneading invariant values; in this study the range is  $[0, 1]$  as  $q = 1/2$ . For each model, one has to figure an optimal value of  $q$ : setting it too small makes the convergence fast so that the tail of the series ( $z$ ) would have a little significance and hence would not differentiate the fine dynamics of the system on longer time scales. Note that  $q = 1/2$  is the largest value that guarantees the one-to-one mapping between the time progression of the separatrix, the symbolic sequence it generates, and the value of kneading invariant,  $K$ .

Given the range and the computational length of the kneading sequence, a colormap of a preset resolution is defined to provide a one-one conversion of each given kneading invariant into the color associated with its numerical value within the given  $[0, 1]$ -range. In this study, the colormap is based on 100 different colors chosen so that any two close kneadings are represented by some contract hues. Specifically, the colormap is defined by a  $100 \times 3$  matrix, in which the three columns correspond to [RGB] values standing for the red, green, and blue colors given by [100], [010] and [001], respectively. The R-column of the colormap matrix has entries linearly decreasing from 1.0 to 0.0, the B-column has entries linearly increasing from 0.0 to 1.0, while any two next entries of the G-column are always 0 and 1 to produce color diversities. So, by the colormap construction, the blue color represents kneading invariants in the  $[0.99, 1.0]$  range, the red color on the opposite side of the spectrum corresponds to kneading invariants in the  $[0, 0.01]$  range, while all other 98 colors fill the spectrum in between. A boundary



between two colors corresponds to a homoclinic bifurcation of the saddle because of a change in the kneading value.

As the result, the obtained color map is sensitive only to variations of the first two decimals of the kneading invariant because the weight of  $q^n$  in (2) decreases quickly as  $n$  increases and due to the resolution of the color map. We can only consider kneading sequences of the length 10, with the contribution of the last entry about  $0.5^{10} \approx 0.001$  to the kneading value. To obtain finer structures of the bifurcation diagram foliated by longer homoclinic loops we can skip some very first kneadings in the 10 entry long episodes: 3-12, 22-31, and so forth. A word of caution: having too much information, i.e., too many bifurcation curves of random colors, will make the bifurcation diagram look noisy on the large areas with an insufficient number of mesh points. Producing clear and informative diagrams for the given system takes time and some amount of experimental work.

## 2. Model of Homoclinic Garden

In our first example, the computational technique based on the symbolic description is used for explorations of dynamical and parametric chaos in a 3D man-made system with the Lorenz attractor, which is code-named the “Homoclinic Garden.”

The Homoclinic Garden (HG) model is described by the following system of three differential equations:

$$\dot{x} = -x + y, \quad \dot{y} = (3 + \mu_1)x + y(1 + \mu_2) - xz, \quad \dot{z} = -(2 + \mu_3)z + xy; \quad (3)$$

with three positive bifurcation parameters,  $\mu$ . An important distinction of Eqs. (3) from the Lorenz equations is the positive coefficient at  $y$  in the second equation. Note that equations with such a term arise e.g. in finite-dimensional analysis of the weakly dissipative Ginzburg-Landau equation near the threshold of the modulational instability.<sup>11</sup>

Equations (3) are  $\mathbb{Z}_2$ -symmetric, i.e.  $(x, y, z) \leftrightarrow (-x, -y, z)$ . In the relevant region of the parameter space the steady states of the system (3) are a saddle at  $x = y = z = 0$ , along with two symmetric saddle-foci at  $x = y = \pm \sqrt{(4 + \mu_1 + \mu_2)(2 + \mu_3)}$ ,  $z = 4 + \mu_1 + \mu_2$ . At  $\mu_3 = 0$  the system (3) possesses the globally attracting two-dimensional invariant surface. If, additionally,  $\mu_2$  vanishes, dynamics upon this surface is conservative, and two homoclinic orbits to the saddle coexist due to the symmetry. On adding the provision  $\mu_1 = 0$ , we observe that two real negative

eigenvalues of the linearization matrix at the saddle are equal. Hence, in the parameter space the codimension-3 point  $\mu_1 = \mu_2 = \mu_3 = 0$  serves as a global organizing center which gives birth to curves of codimension-two homoclinic bifurcations: resonant saddle, orbit-flip and inclination-switch<sup>12</sup> as well as codimension-one bifurcation surfaces corresponding to symmetric homoclinic loops of the origin.

These three primary codimension-two bifurcations were discovered and studied by L.P. Shilnikov in the 60s:<sup>12,13</sup> Either bifurcation of the homoclinic butterfly (Fig. 1) in a  $Z_2$ -system can give rise to the onset of the Lorenz attractor.<sup>14-20</sup> While the model (3) inherits all basic properties of the Lorenz equations, of interest here are two homoclinic bifurcations of saddle equilibria in the phase space of the model, which it was originally designed for. The corresponding bifurcation curves and singularities on

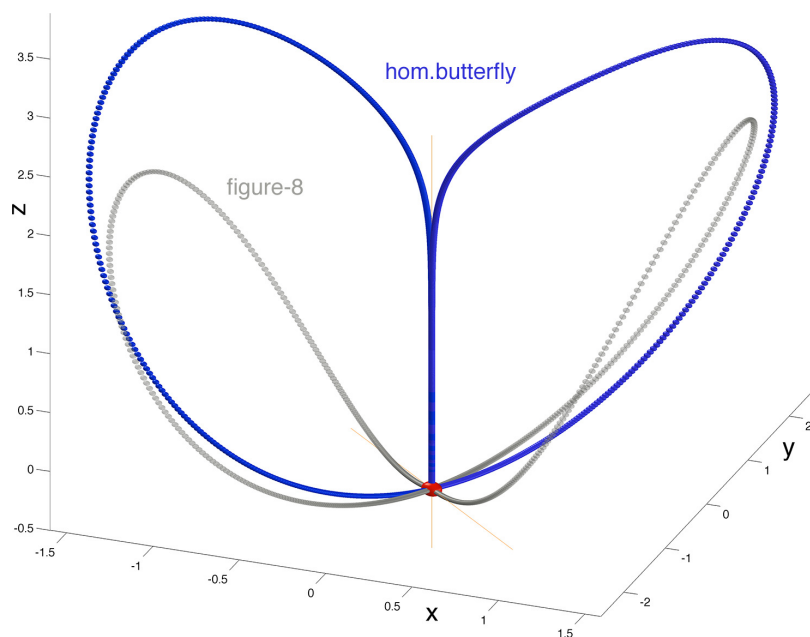


Figure 1. Two types of homoclinic connections to the saddle at origin in the HG model (3). Shown in grey color is the homoclinic figure-8 called so, as the both outgoing separatrices come back to the saddle from the opposite side of the stable leading direction in the  $(x, y)$ -plane. In contrast, the homoclinic butterfly (shown in blue color) is made of the separatrix loops tangent to each other along the leading direction — the  $z$ -axis.

them — codimension-two points globally organize structures of parameter spaces of such  $Zz$ -symmetric systems. As we show below, there is another type of codimension-two points, called Bykov T-points, quintessential for the Lorenz like systems. Such a point corresponds to a closed heteroclinic connection between all three saddle equilibria (Fig. 2) in Eqs. (3): a saddle (at the origin) of the (2,1) type, i.e., with two one-dimensional outgoing separatrices and 2D stable manifold; and two symmetric saddle-foci of the (1,2) type. Such points turn out to cause the occurrence of self-similar, fractal structures in the parameter region corresponding to chaotic dynamics in the most known systems with the Lorenz attractor.<sup>6</sup>

Below, for visualization purposes, we freeze one of the parameters,  $\mu_1$ , to restrict ourselves to the two-parameter consideration of such codimension-two phenomena that give rise to the onset of the Lorenz-type attractors in  $Z_2$ -systems with the homoclinic butterfly (Fig. 1).

A hallmark of any Lorenz-like system is the strange attractor of the emblematic butterfly shape, shown in Fig. 2(a). The eyes of the butterfly wings mark the location of the saddle-foci. The strange attractor of the Lorenz type is structurally unstable<sup>4,21</sup> as the separatrices of the saddle at the origin, filling out the symmetric wings of the Lorenz attractor, bifurcate constantly as the parameters are varied. These separatrices are the primary cause of structural and dynamic instability of chaos in the Lorenz equations and similar models. We say that the Lorenz attractor undergoes homoclinic bifurcation when the separatrices of the saddle change a flip-flop patterns of switching between the butterfly wings centered around the saddle-foci. At such a bifurcation, the separatrices come back to the saddle thereby causing a homoclinic explosion in the phase space.<sup>2,22</sup> The time progression of either separatrix of the origin can be described symbolically and categorized in terms of the number of turns around the symmetric saddle-foci in the 3D phase space (Fig. 2). Alternatively, the problem can be reduced to time evolutions of the  $x$ -coordinate of the separatrix, as shown in panel B of Fig. 2. In the symbolic terms the progression of the  $x$ -coordinate or the separatrix *per se* can be decoded through the binary, (e.g. 1,0) alphabet. Namely, the turn of the separatrix around the right or left saddle-focus, is associated with 1 or 0, respectively. For example, the time series shown in panel B generates the following kneading sequence starting with  $\{1, 0, 1, 1, 1, 1, 1, 0, 1, 0, 0 \dots\}$ , etc. The sequences corresponding to chaotic dynamics will be different even at close parameter values, while they remain the same in a region of regular (robust) dynamics.

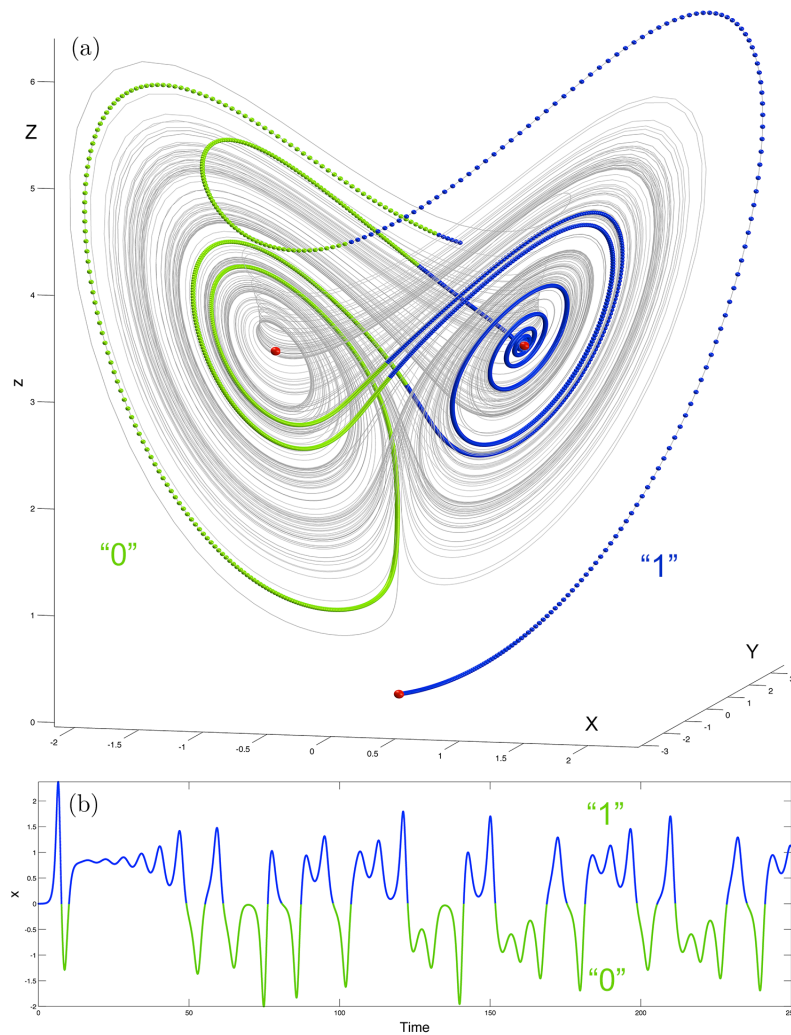


Figure 2. (a) Heteroclinic connection (blue color) between the saddle at the origin and the night saddle-focus (red spheres) overlaid with the chaotic attractor (grey color) in the background in the phase space projection on the HG-model. The progression of the “right” separatrix defines the binary entries,  $\{1, 0\}$ , of kneading sequences, depending whether it turns around the right or left saddle-focus, resp. (b) Time evolutions of the “right” separatrix of the saddle defining the kneading sequence starting with  $\{1, 0, 1, 1, 1, 1, 0, 1, 0, 0 \dots\}$  etc.

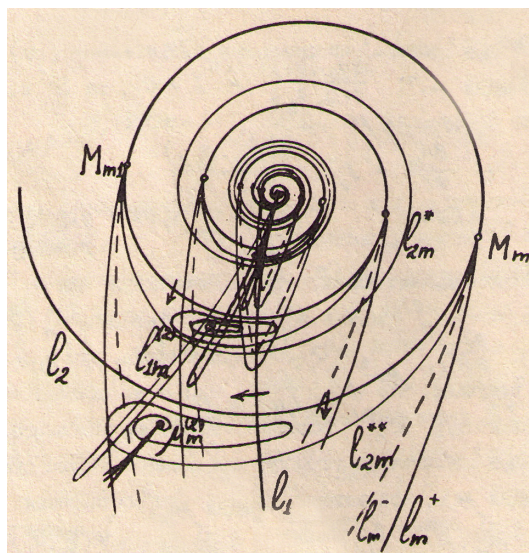


Figure 3. Sketch of a partial bifurcation unfolding of a Bykov T-point of codimension-two corresponding to a heteroclinic connection between the saddle and saddle-focus. It includes spiraling bifurcation curves, each corresponding to a homoclinic bifurcation of the saddle such that the number of turns of the separatrix around the saddle-focus increments with each turn of the spiral accumulating to the T point. Straight line originating from the T-point corresponds to homoclinics of the saddle-focus. Points (labeled by  $M$ 's) on the primary spiral corresponding to inclination-switch homoclinic bifurcations of the saddle give rise to saddle-node and period-doubling bifurcations of periodic orbits of the same symbolic representations. The primary T-points give rise to countably many subsequent ones with similar bifurcations structures in the parameter plane. Courtesy of V. Bykov.<sup>5</sup>

Figure 3 sketches a partial bifurcation unfolding of a heteroclinic bifurcation corresponding to a closed connection between one saddle-focus and one saddle whose one-dimensional stable and unstable, resp., separatrices merge at the codimension-two T-point in the parametric plane.<sup>5,23,26</sup> Its center piece is a bifurcation curve spiraling onto the T-point. This curve corresponds to a homoclinic loop of the saddle such that the number of turns of the separatrix around the saddle-focus increments with each turn of the spiral approaching to the T-point. The straight line,  $l_1$ , originating from the T-point corresponds to homoclinics of the saddle-focus satisfying the Shilnikov condition,<sup>27,28</sup> and hence leading to the existence of denumerable set of saddle periodic orbits nearby.<sup>29</sup> Turning points (labelled by  $M$ 's) on the primary spiral correspond to inclination-switch homoclinic bifurcations

of the saddle.<sup>12,19</sup> Each such a homoclinic bifurcation point gives rise to the occurrence of saddle-node and period-doubling bifurcations (on curves  $L_m^+$  and  $L_m^-$ ) of periodic orbits of the same symbolic representation. The central T-point gives rise to countably many subsequent ones with similar bifurcations structures on smaller scales in the parameter plane. The indicated curves in the unfolding by Bykov, retain in the  $\mathbb{Z}_2$ -symmetric systems too<sup>23,30</sup> in addition to new one due to the symmetry.

At the first stage of the pilot study of the HG-model, we performed a bi-parametric,  $(\mu_2, \mu_3)$ , scan of Eqs. (3) using the first 10 kneadings. This colormap of the scan is shown in Fig. 4. In this diagram, a particular color in the spectrum is associated with a persistent value of the kneading invariant on a level curve. A window of a solid color corresponds to a constant kneading invariant, i.e. to simple dynamics in the system. In such windows simple attractors such as stable equilibria or stable periodic orbits dominate the dynamics of the model. A borderline between two solid-color regions corresponds to a homoclinic bifurcation through a boundary, which is associated with a jump between the values of the kneading invariant. So, the border between the blue (the kneading invariant  $K = 1$ ) and the red ( $K = 0$ )

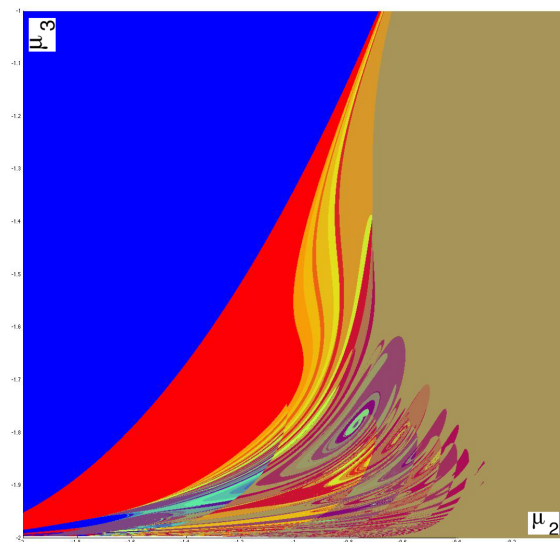


Figure 4. Pilot bi-parameter sweeping of the HG-model using the very first 10 kneadings at  $\mu_1 = 0$ . Solid colors correspond to regions of simple dynamics. Multicolored regions fill out the chaos land. The borderline between red and the blue regions corresponds to the primary homoclinic butterfly bifurcation in Fig. 1 and begins from the origin in the parameter plane.



regions corresponds to the bifurcation of the primary homoclinic butterfly (Fig. 1). The brown region is dominated by the stable periodic orbit, coded with two symbols  $[1, 0]$ . The pilot scan clearly indicates the presence of the complex dynamics in the model. A feature of the complex, structurally unstable dynamics is the occurrence of numerous homoclinic bifurcations, which are represented by border lines of various colors that foliate the corresponding region in the bi-parametric scan. One can note the role of the codimension-two orbit-flip bifurcation<sup>12</sup> at  $\mu_1 = \mu_2 = 0$  in shaping the bifurcation diagram of the model. Observe that the depth (10 kneadings) of the scanning can only reveal homoclinic trajectories/bifurcations up to the corresponding configurations/complexity.

Figure 5 represents a high-resolution scan of the complex dynamics of the HG-model, using the same  $[5-15]$  kneadings. It is made of 16

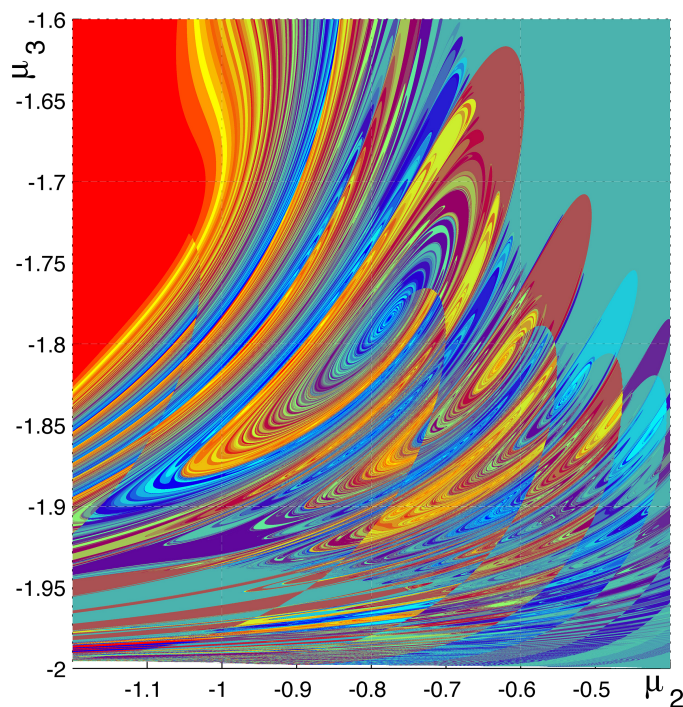


Figure 5. High resolution,  $[5-15]$  kneading-range scan of dynamics of the HG-model showing a complex fractal structure of the parameter space. Centers of swirls correspond to heteroclinic T-points of codimension-2. The scan is made of 16 panels, each with  $[10^3 \times 10^3]$  mesh points. One color curve corresponds to a homoclinic bifurcation of the saddle at the origin.

panels, each one with  $10^3 \times 10^3$  mesh points. This diagram is a de facto demonstration of this computational technique. This color scan reveals a plethora of T-points as well as the saddles separating swirling structures. One can see that the diagram reveals adequately the fine bifurcation structures of the Bykov T-points.<sup>5</sup> The structure of the bi-parametric scan can be enhanced further by examining longer tails of the kneading sequences. This allows for the detection of smaller-scale swirling structures within the larger scrolls, as predicted by the theory.

### 3. Lorenz Model: Primary and Secondary T-points

The Lorenz equation<sup>1</sup> from hydrodynamics is a system of three differential equations:

$$\dot{x} = -\sigma(x - y), \quad \dot{y} = rx - y - xz, \quad \dot{z} = -\frac{8}{3}z + xy, \quad (4)$$

with positive parameters:  $\sigma$  being the Prandtl number quantifying the viscosity of the fluid, and  $r$  being a Rayleigh number that characterizes the fluid dynamics. Note that Eqs. (4) are  $\mathbb{Z}_2$ -symmetric, i.e.  $(x, y, z) \leftrightarrow (-x, -y, z)$ .

The primary codimension-two T-point at  $(r = 30.38, \sigma = 10.2)$  corresponding to the heteroclinic connections between the saddle and saddle-foci (shown in Fig. 6) in the Lorenz equation was originally discovered by Petrovskaya and Yudovich.<sup>31</sup> They initially conjectured that its bifurcation unfolding would include concentric circles, not spirals, corresponding to bifurcation curves for homoclinic loops of  $\{1, [0]^{(k)}\}$  symbolic representations, with quite large  $k$  ( $\geq 40$ ). Figure 7 represents the  $(r, \sigma)$  kneading scans of the dynamics of the Lorenz equation near the primary T-point. In the scan, the red-colored region corresponds to a “pre-turbulence” in the model, where chaotic transients converge eventually to stable equilibria. The borderline of this region corresponds to the onset of the strange chaotic attractor in the model. The lines foliating the fragment of the parameter plane correspond to various homoclinic bifurcations of the saddle at the origin. Observe the occurrence of a saddle point in the parameter plane that separates the bifurcation curves that winds onto the T-point from those flowing around it. Locally, the structure of the T-point and a saddle recalls a saddle-node bifurcation. Note too that likewise trajectories of a planar system of ODEs, no two bifurcation curves can cross



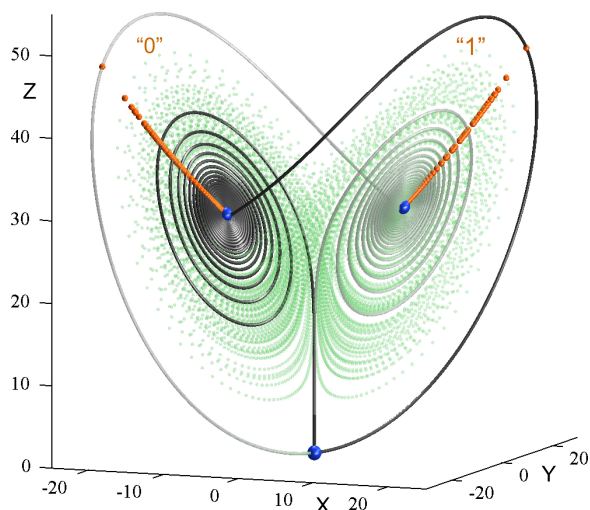


Figure 6. Primary heteroclinic connections between the saddle and two saddle-foci (indicated by the blue spheres) in the Lorenz model at  $(r = 30.38, \sigma = 10.2)$  corresponding to the primary Bykov T-point in the parameter space for  $b = 8/3$ . The strange attractor is shaded in light green colors. The secondary T-point in the Lorenz model is similar to that depicted in Fig. 2 for the Eqs. (3).

or merge unless at a singularity, as they correspond to distinct homoclinic loops of the saddle.

By construction, the scans based on the kneading episodes, resp. [11–61], and combined [11–61] and [26–36] ranges, shown in Fig. 7, let us reveal the sought homoclinic bifurcations and the homoclinic connections of the saddle of the desired lengths. Homoclinic connections that are shorter or longer than the given range will be either represented by solid stripes, or produce “noisy” regions where the resolution (the number of the mesh points) of the scan is not good enough to expose fine details due to the abundance of data information.

Next let us examine the kneading-based scan of the dynamics of the Lorenz equation near the secondary Bykov T-point at  $(r = 85, \sigma = 11.9)$  shown in Fig. 8. The corresponding heteroclinic connection looks alike that shown in Fig. 2 for the HG-model (3). Besides the focal point *per se*, the scan reveals a plethora of subsequent T-points corresponding to more complex heteroclinic connections between the saddle and saddle-foci. It is the dynamics due to that saddle-foci that give rise to such

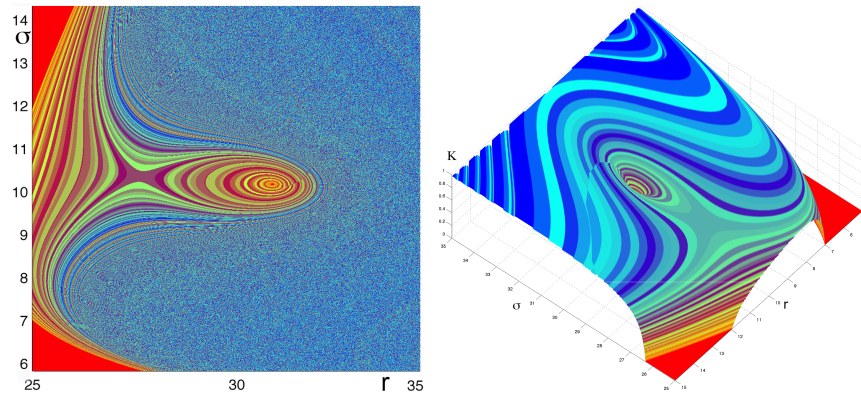


Figure 7. Bi-parametric scans, 2D and 3D, of different depths of the Lorenz equation around the primary T-point at  $(r = 30.38, \sigma = 10.2)$ . Solid red region corresponds to the kneading sequence  $\{1, [0]^\infty\}$  generated by the separatrix converging to the stable focus in the phase space. (left) Combined scan using two kneading ranges, [11–61] and [26–36], reveals the structure of homoclinic bifurcations in a vicinity of the primary T-point. The scan creates an illusion that the bifurcation unfolding contains concentric circles rather than weakly converging spirals due to long lengths of the homoclinic connections. Note a saddle point separating the bifurcations curves (blueish colors) that are supposed to end up at the T-points from those flowing around it on the right and left. (right) 3D kneading scan of the [11–61]-range with the primary T-point in the deep potential dwell (at the level  $K=0$ ), and a saddle point. One can notice that locally, this pattern in the *parameter plane* resembles of a typical setup for saddle-node bifurcations.

vertices and make bifurcation structures become fractal and self-similar. The complexity of the bifurcation structure of the Lorenz-like systems is a perfect illustration of the dynamical paradigm of so-called quasi-chaotic attractors introduced and developed by L.P. Shilnikov within the framework of the mathematical Chaos theory.<sup>32–36</sup> Such a chaotic set is impossible to parameterize and hence to fully describe its multi-component structure due to dense complexity of ongoing bifurcations occurring within it.

Figure 9 represents the magnification of a vicinity of the secondary T-point, which is scanned using [10–18] kneadings. The magnification reveals finer structures of the bifurcation unfolding, like one derived analytically by Bykov in Fig. 3. Of special interest here are a few smaller-scale spirals visibly located between the consecutive scrolls around the secondary T-point, that terminate the bifurcation curves starting from the codimension-two inclination switch bifurcations.

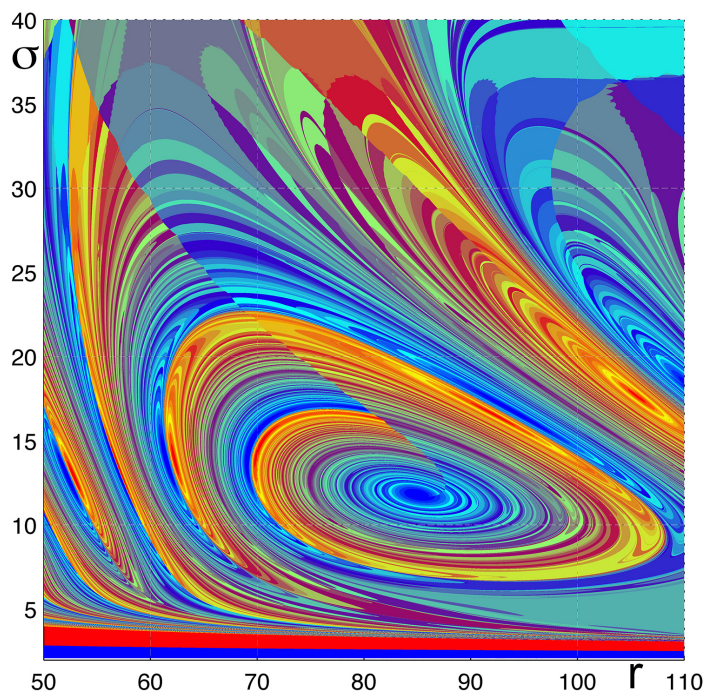


Figure 8. Bi-parametric sweeping of the Lorenz equation around the primary T-point at  $(r = 85, \sigma = 11.9)$  using [6–16] kneadings, revealing a plethora of subsequent T-points giving rise to self-similar fractals in the parameter space of the structurally unstable chaotic attractor. The corresponding heteroclinic connections look alike one shown in Fig. 2 for the HG-model (3).

#### 4. Summary

The paper highlights the key and the universal principles of chaotic dynamics in deterministic systems with the Lorenz-like attractors. It shades the light on the role of homoclinic and heteroclinic bifurcations as emergent centers for pattern formations in parameter spaces corresponding to complex dynamics.

The symbolic methods will benefit studies of systems supporting adequate symbolic partitions. Our experiments with the kneading scans of several Lorenz-like systems have unambiguously revealed a wealth of multi-scale swirl and saddle structures in the intrinsically fractal regions in the parameter planes corresponding to strange chaotic attractors. There is still a room for improvement of the computational tools aimed at understanding

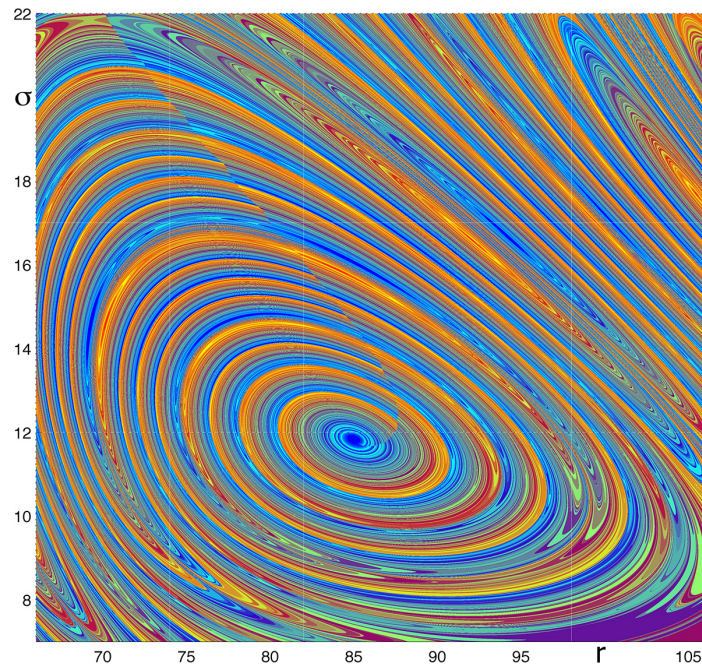


Figure 9. Magnification of the bi-parametric [10–18] kneading-range sweeping a vicinity of the secondary T-point at  $(r = 85, \sigma = 11.9)$  shows a fine structure if its bifurcation infolding similar to that analytically found by Bykov (compare with Fig. 3).

in detail a variety of global mechanisms giving rise to fractal structures in bi-parametric scans of systems with other strange attractors. The study is a leap forward to fully disclose the most of basic mechanisms giving rise to generic self-similar structures in a variety of systems of diverse origins.

### Acknowledgments

This work was in part supported by the NSF grant DMS-1009591, and RFFI 11-01-00001, and by the grant in the agreement of August 27, 2013 No.02.B.49.21.003 between the Ministry of Education and Science of the Russian Federation and Labachersky State University of Nizhni Nougorod. We would like to thank J. Schwabedal and R. Barrio for helpful discussions, and R. Clewley for his guidance on the PyDSTool package<sup>37</sup> used for computer simulations.



## References

1. E. Lorenz, Deterministic nonperiodic flow, *J. Atmospheric Sci.* **20**, 130–141 (1963).
2. V. Afraimovich, V. V. Bykov, and L. P. Shilnikov, The origin and structure of the Lorenz attractor, *Sov. Phys. Dokl.* **22**, 253–255 (1977).
3. L. Shilnikov, Bifurcation theory and the Lorenz model, *Appendix to Russian edition of “The Hopf Bifurcation and Its Applications.”* Eds. J. Marsden and M. McCracken. pp. 317–335 (1980).
4. V. Afraimovich, V. V. Bykov, and L. P. Shilnikov, On structurally unstable attracting limit sets of Lorenz attractor type, *Trans. Moscow Math. Soc.* **44**(2), 153–216 (1983).
5. V. V. Bykov, On the structure of bifurcations sets of dynamical systems that are systems with a separatrix contour containing saddle-focus, *Methods of Qualitative Theory of Differential Equations, Gorky University (in Russian)*. pp. 44–72 (1980).
6. R. Barrio, A. Shilnikov, and L. Shilnikov, Kneadings, symbolic dynamics, and painting Lorenz chaos, *Inter. J. Bif. Chaos.* **22**(4), 1230016–1230040 (2012).
7. J. Milnor and W. Thurston, On iterated maps of the interval, *Lecture Notes in Math.* **1342**, 465–563 (1988).
8. D. Rand, The topological classification of Lorenz attractors, *Mathematical Proceedings of the Cambridge Philosophical Society.* **83**(03), 451–460 (1978).
9. M. Malkin, Rotation intervals and dynamics of Lorenz type mappings, *Selecta Math. Sovietica.* **10**, 265–275 (1991).
10. C. Tresser and R. Williams, Splitting words and Lorenz braids, *Physica D: Nonlinear Phenomena.* **62**(1–4), 15–21 (1993).
11. B. A. Malomed and A. A. Nepomnyashchy, Onset of chaos in the generalized Ginzburg-Landau equation, *Phys. Rev. A.* **42**, 6238–6240 (1990).
12. L. P. Shilnikov, A. L. Shilnikov, D. Turaev, and L. O. Chua, *Methods of qualitative theory in nonlinear dynamics. Part I and II.* World Scientific Publishing Co. Inc. (1998, 2001).
13. L. Shilnikov, On the birth of a periodic motion from a trajectory bi-asymptotic to an equilibrium state of the saddle type, *Soviet Math. Sbornik.* **35**(3), 240–264 (1968).
14. L. Shilnikov, The theory of bifurcations and quasiattractors, *Uspeh. Math. Nauk.* **36**(4), 240–242 (1981).
15. A. Shilnikov, Bifurcations and chaos in the Marioka-Shimizu model. Part I, *Methods in qualitative theory and bifurcation theory (in Russian)*. pp. 180–193 (1986).
16. C. Robinson, Homoclinic bifurcation to a transitive attractor of Lorenz type., *Nonlinearity.* **2**, 495–518 (1989).
17. M. Rychlic, Lorenz attractor through Shil’nikovtype bifurcation I., *Erof. Theory and Dyn. Systems.* **10**, 793–821 (1990).
18. A. Shilnikov, On bifurcations of the Lorenz attractor in the Shimizu-Morioka model, *Physica D.* **62**(1–4), 338–346 (1993).

19. A. L. Shilnikov, L. P. Shilnikov, and D. V. Turaev, Normal forms and Lorenz attractors, *Inter. J. Bif. Chaos.* **3**(5), 1123–1139 (1993).
20. D. Lyubimov and S. Byelousova, Onset of homoclinic chaos due to degeneracy in the spectrum of the saddle, *Physica D: Nonlinear Phenomena.* **62**(1–4), 317–322 (1993).
21. J. Guckenheimer and R. F. Williams, Structural stability of Lorenz attractors, *Inst. Hautes Études Sci. Publ. Math.* **50**(50), 59–72 (1979).
22. J. L. Kaplan and J. A. Yorke, Preturbulence: a regime observed in a fluid flow model of Lorenz, *Comm. Math. Phys.* **67**(2), 93–108 (1979).
23. V. V. Bykov, The bifurcations of separatrix contours and chaos, *Physica D.* **62**(1–4), 290–299 (1993).
24. J. S. Nicolis, G. Mayer-Kress and G. Haubs, Non-uniform chaotic dynamics with implications to information processing, *Zeitschrift für Naturforschung A.* **38**(11), 1157–1169 (1983).
25. J. S. Nicolis, Chaos and Information Processing: A Heuristic Outline, *World Scientific Press* (1991).
26. P. Glendinning and C. Sparrow, T-points: a codimension two heteroclinic bifurcation, *J. Stat. Phys.* **43**(3–4), 479–488 (1986).
27. L. P. Shilnikov, A case of the existence of a countable number of periodic motions, *Sov. Math. Dokl.* **6**, 163 (1965).
28. L. Shilnikov and A. Shilnikov, Shilnikov bifurcation, *Scholarpedia.* **2**(8), 1891 (2007).
29. L. Shilnikov, The existence of a denumerable set of periodic motions in four-dimensional space in an extended neighborhood of a saddle-focus., *Soviet Math. Dokl.* **8**(1), 54–58 (1967).
30. P. Glendinning and C. Sparrow, Local and global behavior near homoclinic orbits, *J. Stat. Phys.* **35**(5–6), 645–696 (1984).
31. N. Petroskaya and V. Yudovich, Homoclinic loops on the Saltzman-Lorenz system, *Methods of Qualitative Theory of Differential Equations, Gorky University.* pp. 73–83 (1980).
32. V. S. Afraimovich and L. P. Shilnikov. Strange attractors and quasiattractors. In *Nonlinear dynamics and turbulence*, Interaction Mech. Math. Ser., pp. 1–34. Pitman, Boston, MA (1983).
33. S. V. Gonchenko, L. P. Shil'nikov, and D. V. Turaev, Dynamical phenomena in systems with structurally unstable Poincare homoclinic orbits, *Chaos.* **6**(1), 15–31 (1996).
34. L. Shilnikov, Mathematical problems of nonlinear dynamics: A tutorial. Visions of nonlinear mechanics in the 21st century, *Journal of the Franklin Institute.* **334**(5–6), 793–864 (1997).
35. D. Turaev and L. Shilnikov, An example of a wild strange attractor, *Sbornik. Math.* **189**(2), 291–314 (1998).
36. L. Shilnikov, Bifurcations and strange attractors, *Proc. Int. Congress of Mathematicians, Beijing(China) (Invited Lectures).* **3**, 349–372 (2002).
37. S. W. L. M. Clewley, R. H. and J. Guckenheimer. Pydstool: an integrated simulation, modeling, and analysis package for dynamical systems. Technical report, <http://pydstool.sourceforge.net> (2006).